Results in Chemistry 27 (2026) 103415

Contents lists available at ScienceDirect

Brazilian Journal of Health and Clinical Approaches

journal homepage: www.sciencedirect.com/journal/bjhca

Discovery of a new GLP-1 receptor agonist using DNA encoded-libraries and similarity search

Ju Ho Lee [a,d,1], Doyoun Kim [a,b,d,1], Hyejin Jeon [c,1], Sung Bum Park [a,d,1], Byumseok Koh [a,b,d,1], Byungho Lim [a,b,d,1], Kyeong A. Lee [a,d], Kyoung Jin Choi [a,d], Seong Soon Kim [a,d], Yujin Kwon [a,b,d], Jung-Hee Lim [a,d], Jung Hyun Jo [a,d], Yeonji Park [a,d], Sunjong Yu [a,d], Nam-Chul Cho [a,d], Wan Namkung [c,*], Yuno Lee [a,d,**], Hyun Jin Kim [a,d,**], Ki Young Kim [a,d,**], Jung-Nyoung Heo [a,d,**]

[a] Therapeutics & Biotechnology Division, Korea Research Institute of Chemical Technology (KRICT), Daejeon 34114, Republic of Korea
[b] Medicinal Chemistry & Pharmacology, Korea National University of Science & Technology (UST), Daejeon 34113, Republic of Korea
[c] College of Pharmacy and Yonsei Institute of Pharmaceutical Sciences, Yonsei University, Incheon 21983, Republic of Korea
[d] Department of DEL Technology, KRICT, Daejeon 34114, Republic of Korea

ARTICLE INFO

Keywords:
DNA-encoded libraries
DEL
GLP-1R
Drug screening
Diabetes
Obesity

ABSTRACT

The glucagon-like peptide-1 receptor (GLP-1R) is a validated therapeutic target for type 2 diabetes and obesity, yet discovery of orally available small-molecule agonists remains challenging. Here, we applied DNA-encoded library (DEL) technology to identify novel small-molecule binders and functional agonists of GLP-1R. Screening of DEL against recombinant GLP-1R revealed recurring structural motifs, particularly a chromane-containing building block. Selected high-scoring off-DNA compounds were synthesized and further expanded through similarity-based searches.

Functional evaluation using a cAMP assay in GLP-1R–expressing CHO-K1 cells identified KCB-C06 as a GLP-1R agonist that induced a receptor-specific, dose-dependent increase in intracellular cAMP. Direct binding of KCB-C06 to GLP-1R was confirmed by biolayer interferometry. Structure-based analyses revealed that KCB-C06 occupies an orthosteric pocket partially overlapping with known small-molecule agonists, engaging key hydrophobic and aromatic residues through π-stacking and backbone interactions.

Study demonstrates that DEL screening combined with similarity analysis, biophysical validation, and structure-guided modeling can uncover novel small-molecule GLP-1R agonists. These findings provide a foundation for subsequent structure–activity relationship optimization toward small-molecule based GLP-1R therapeutics.

1. Introduction

GLP-1R is a class B G-protein–coupled receptor that plays a central role in metabolic regulation [1,2]. Activated by the incretin hormone GLP-1, GLP-1R stimulates insulin secretion, suppresses glucagon release, delays gastric emptying, and promotes satiety, thereby contributing to glucose homeostasis and energy balance [3,4]. These pleiotropic effects make GLP-1R a critical therapeutic target in type 2 diabetes mellitus and obesity, with agonists demonstrating robust efficacy in improving glycemic control, reducing body weight, and lowering cardiovascular risk [1,5,6].

Beyond metabolic regulation, increasing evidence highlights broader physiological roles for GLP-1R, including neuroprotection, cardioprotection, and modulation of inflammation [6,7]. Expression of GLP-1R in the central nervous system suggests a direct influence on appetite regulation, learning, and memory, while its presence in

* Corresponding author.
** Corresponding authors at: Therapeutics & Biotechnology Division, Korea Research Institute of Chemical Technology (KRICT), Daejeon 34114, Republic of Korea.
E-mail addresses: wnamkung@yonsei.ac.kr (W. Namkung), yunolee1@krict.re.kr (Y. Lee), hyunjin@krict.re.kr (H.J. Kim), kykim@krict.re.kr (K.Y. Kim), heojn@krict.re.kr (J.-N. Heo).
[1] Equally contributed.

https://doi.org/10.1016/j.rechem.2026.103415
Received 23 February 2026; Accepted 7 May 2026
Available online 7 May 2026

peripheral tissues such as the heart, kidney, and gastrointestinal tract indicates systemic impact [8]. The expanding clinical applications of GLP-1R agonists underscore the significance of this receptor not only as a metabolic regulator but also as a potential therapeutic entry point for neurodegenerative and cardiovascular diseases [9–11]. However, the discovery of novel small-molecule modulators for complex GPCRs like GLP-1R remains a significant challenge, necessitating powerful and innovative screening platforms.

DEL technology has emerged as a powerful platform for the discovery of novel small-molecule therapeutics [12–14]. DELs consist of vast collections of compounds, each covalently linked to a unique DNA barcode that serves as a molecular identifier [15–17]. This encoding strategy enables the synthesis, storage, and high-throughput screening of billions of compounds in a pooled format, far exceeding the scale achievable by traditional small-molecule libraries [18]. By combining combinatorial chemistry with DNA sequencing, DEL technology allows efficient identification of high-affinity binders to protein targets with exceptional sensitivity and throughput.

DEL technology is significantly early-stage screening and expands chemical diversity at a fraction of the cost and time required for conventional methods [19]. DEL-based approaches have already yielded candidate molecules against challenging targets, including protein–-protein interactions and enzymes previously considered "undruggable" [[20–22]]. Moreover, the integration of DELs with structural biology, computational chemistry, and fragment-based drug design enhances hit validation and optimization [21,22]. DELs are therefore increasingly recognized as a transformative tool for modern drug discovery pipelines, bridging the gap between target identification and clinical lead development.

In this study, we leveraged DEL technology to identify novel small-molecule binders of GLP-1R. Our aim was to discover compounds capable of modulating its activity. Such an approach not only expands the chemical space of potential GLP-1R-targeted agents but also provides an opportunity to develop therapeutics with distinct pharmacological properties compared to peptide-based agonists, thereby addressing unmet needs in metabolic and related diseases.

2. Materials and methods

2.1. DEL binding assay

DEL binding assay was performed using the DyNAbind® 10 Million Compound DNA-Encoded Library Kit (Merck, #DYNA002-5VL, Darmstadt, Germany) according to the manufacturer's instructions, with minor modifications in buffer composition and protein quality control (QC) procedures. Recombinant GLP-1R protein (R&D Systems, Minneapolis, MN, USA) was used as the target. The workflow consisted of four main steps: protein immobilization, bead preparation and binding, protein QC, and DEL binding. For protein immobilization, His-tagged GLP-1R protein was immobilized on Ni-NTA magnetic beads (Thermo Fisher Scientific, Waltham, MA, USA). Selection buffer (50 mM Tris-HCl, pH 8.0, 150 mM NaCl, 10 mM imidazole, 0.1 mg/mL salmon sperm DNA, and 0.05% Tween-20) and elution buffer (50 mM Tris-HCl, pH 8.0, 150 mM NaCl, and 0.05% Tween-20) were freshly prepared. For bead preparation and protein binding, Magnetic beads were activated at room temperature for 5 min and washed three times with 300 μL of selection buffer using vortexing and magnetic separation. After washing, beads were resuspended in 125 μL of selection buffer, and a 25 μL aliquot was set aside as the "Blank bead" control. The remaining beads were used for protein binding. For immobilization, 6 μg of GLP-1R protein was diluted in 120 μL of selection buffer. A 20 μL fraction of this solution was reserved as the "Input" sample, while the remaining 100 μL was added to the bead suspension and mixed thoroughly. Binding was carried out by rotating the bead–protein mixture at room temperature for 2 h. After incubation, the beads were magnetically separated, and the supernatant was collected as the "Flow-through." Beads were washed once with 100 μL of selection buffer, and the wash supernatant was collected as the "Wash" sample. Elution was performed with 100 μL of elution buffer by pipetting 10 times, and 50 μL of eluate was collected ("Elution"). The remaining bead suspension was incubated at 95 °C for 10 min, magnetically separated, and the supernatant collected as "Heated Elution." Finally, beads were resuspended in 50 μL of selection buffer and stored as "Heated Bead." To confirm GLP-1R immobilization, samples were analyzed by SDS-PAGE using a NuPAGE 4–12% Bis-Tris gel (Invitrogen, Carlsbad, CA, USA) followed by Coomassie Brilliant Blue R-250 staining (Bio-Rad, USA). Gels were imaged with a ChemiDoc chemiluminescence imaging system (Bio-Rad, USA). For the DEL binding assay, 20 μL of His-tag pulldown beads were washed three times with selection buffer and incubated with 20 μg of GLP-1R protein for 2 h at room temperature under gentle rotation (20 rpm) to allow immobilization. Protein-bound beads were then incubated with 100 μL of the Merck DEL library at room temperature for 2 h with continuous mixing (20 rpm) to enable compound–protein binding.

2.2. Off-DNA chemical synthesis

Off-DNA compounds (compound **1a-6b**) selected from DEL screening data for GLP-1R were synthesized using general peptide coupling procedure in Scheme S1-S3. Boc-amino acid (1 equiv) was coupled using HATU (1.2 equiv) and DIPEA (4 equiv) in DCM at room temperature for 16 h. After analysis of TLC and the reaction was completed, H_2O was added for dilution and then extraction with DCM for 3 times. The combined organic layers were washed with brine and dried over Na_2SO_4. After filtration and concentration of the crude in vacuo, the product was purified by silica gel column chromatography eluting with DCM and Ethyl acetate (0 to 80% EtOAc).

The C-terminal end of tripeptide was modified through esterification, ester hydrolysis, introduction of *N*-methyl amine following the protocol in the experimental method of Supplementary Information.

2.3. The Binding kinetic analysis of hit compound by Biolayer Interferometry (BLI)

The recombinant human GLP-1 receptor was purchased from Bio-Techne (Minneapolis, MN, USA). For immobilizing recombinant protein on the surface of the super streptavidin biosensor (Sartorius, Gottingen, Germany) to measure the binding kinetics between hit compounds and GLP-1R, the 5 μg of GLP-1R was mixed with 20 times molar concentration of NHE-PEG4-Biotin, which stocked in 20 mM concentration (Thermo Fisher Scientific) and incubated at 25 °C for an hour. The Biolayer interferometric sensor gram for binding kinetic analysis were measured under Octet R8 (Sartorius). The parameters for protein immobilization, base line, association, and dissociation time set as 30, 300, 60, 300, and 300 s, respectively. All measurements were reacted in buffer 1× PBS-P (Cytiva, Marlborough, MA, USA) in black bottom 96 well plate (BRANDtech, Essex, CT, USA). The binding kinetic sensor gram were then fit by heterogenous analyte binding mode for global fitting option in Octet analysis software (version 2.1, Sartorius).

2.4. Binding mode prediction of GLP-1R in complex with hit compounds

To predict the unbiased binding mode of the hit compound against the GLP-1R, the artificial intelligent (AI) based diffusion prediction conducted with the amino acid sequence corresponds human GLP-1R (uniprot ID P43220) into chai-1 software [23]. For the accurate binding mode prediction, the corresponding protein part of the experimental cryoEM structure of GLP-1R in complex with danuglipron (PF-06882961), which is an oral GLP-1R agonist from Pfizer (PDB ID 7LCJ) [24] was used for the docking study as a receptor. A grid box set up with dimensions of 45.7 × 27.3 × 36.4 Å centered at 124.9, 162.3, 114.2 Å with seed number as 100 and exhaustiveness as 12 and docking simulation were conducted using Autodock vina software [25]. The

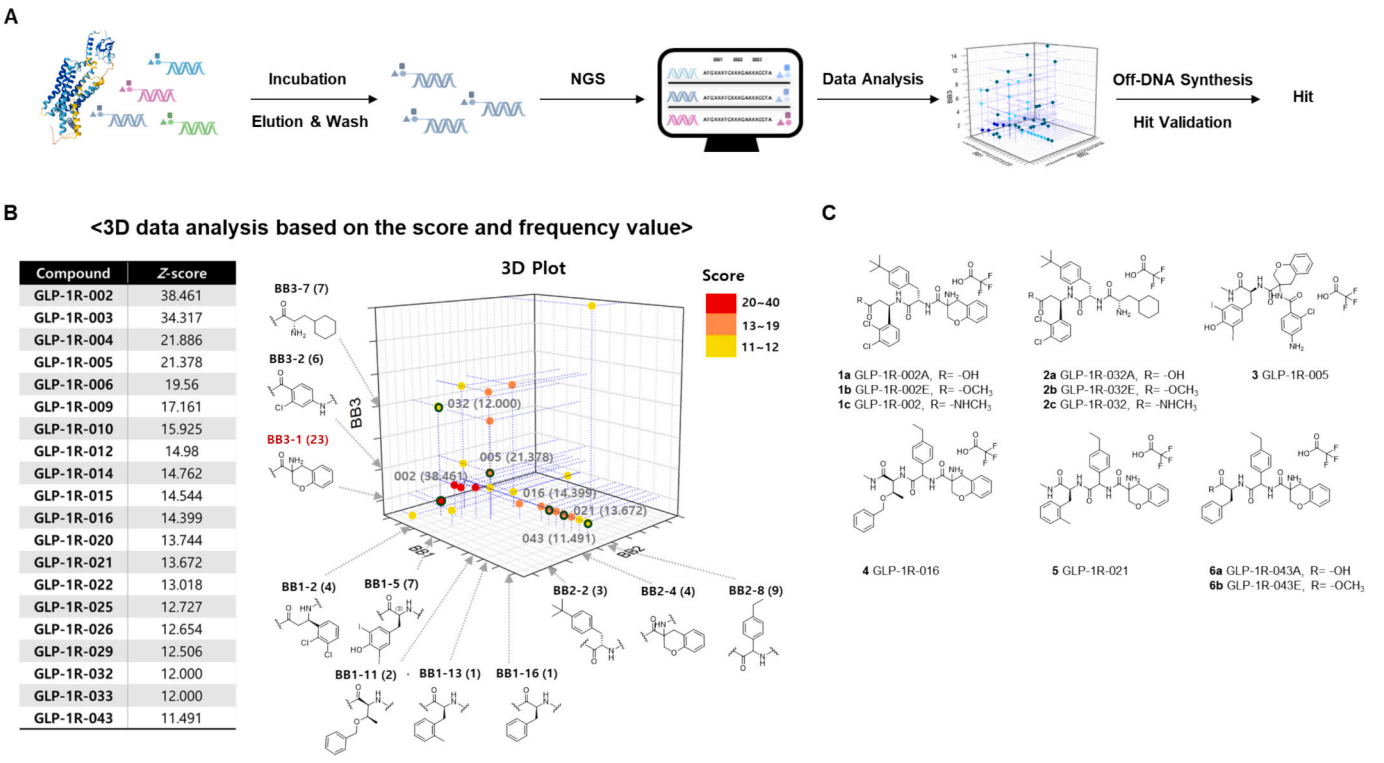

Compound	*Z*-score
GLP-1R-002	38.461
GLP-1R-003	34.317
GLP-1R-004	21.886
GLP-1R-005	21.378
GLP-1R-006	19.56
GLP-1R-009	17.161
GLP-1R-010	15.925
GLP-1R-012	14.98
GLP-1R-014	14.762
GLP-1R-015	14.544
GLP-1R-016	14.399
GLP-1R-020	13.744
GLP-1R-021	13.672
GLP-1R-022	13.018
GLP-1R-025	12.727
GLP-1R-026	12.654
GLP-1R-029	12.506
GLP-1R-032	12.000
GLP-1R-033	12.000
GLP-1R-043	11.491

Fig. 1. Workflow of DEL screening, data analysis and hit validation. (A) DEL screening for hit discovery of GLP-1R. (B) 3D plot of building blocks (BB1-BB3) derived from top 50 of score value. 3D scatter plot was visualized using Origin Pro 8.5. The colour of each dot (red, orange, or yellow) and parentheses next to the label of off-DNA compounds indicates each score value. The parentheses next to the label of building blocks indicates each frequency value. (C) The structure of GLP-1R off-DNA compounds. (For interpretation of the references to colour in this figure legend, the reader is referred to the web version of this article.)

interaction analysis by using interaction design tool in SAMSON software packages (Version 2025-R3) [26]. The binding free energy were then calculated by using PRODIGY web server [27]. In addition, to predict the structural selectivity, the crystal structure of apo-form GLP-1R (PDB 6LN2) [28] was used with the grid box 41.2 × 39.8 × 46.0 Å centered at 20.6, 27.3, 61.8 Å. All structural figures were prepared by chimera-x software (version 1.8) [29].

2.5. Cell culture & cAMP assay

CHO-K1 cells stably expressing GLP-1R were cultured in Dulbecco's Modified Eagle's Medium (DMEM; Welgene Inc., Gyeongsan, Korea) supplemented with 10% fetal bovine serum (FBS) and 1% penicillin/streptomycin at 37 °C in a humidified atmosphere containing 5% CO_2. Cells were seeded into 96-well plates at a density designed to achieve approximately 80% confluency the following day. After 24 h of incubation, cells were treated with test compounds at various concentrations for 10 min. All compounds were dissolved in dimethyl sulfoxide (DMSO) with a final concentration of 1% (*v*/v). Exendin-4 (10 nM) served as a positive control, while vehicle control cells were treated with 1% DMSO alone. Intracellular cAMP levels were quantified using the cAMP-Glo™ Assay kit (Promega, Madison, WI, USA) according to the manufacturer's instructions. Luminescence was measured using an Infinite M200 microplate reader (Tecan, Männedorf, Switzerland).

2.6. Statistical analysis

All graphical results are expressed as means with standard deviation of the mean ± standard deviation (SD). Statistical analyses were performed using GraphPad Prism software (GraphPad Software Inc., La Jolla, CA, USA). Statistical significance was determined using multiple t-tests or a one-way ANOVA followed by Tukey's multiple comparison test. $P < 0.05$ was considered statistically significant.

3. Results

3.1. Selection and synthesis of Off-DNA compounds from DEL screening

DELs were used to identify high-affinity GLP-1R binders. Analysis of data from DEL screening for GLP-1R is a critical process to select off-DNA compounds for hit discovery (Fig. 1A) [30–32]. Off-DNA compounds were selected through 3D analysis of NGS data. We selected GLP-1R off-DNA compounds with high score and frequency value, which are important indicators for potential binder. After enumeration of the building blocks of DEL, the structure of non-specific binder as false-positive or undruggable moiety like trityl group were excluded. The histogram and 3D plot indicated that the 3-aminochromane-3-carboxylic acid (BB3–1) at the N-terminal end of a tripeptide had a notably high frequency ($n = 23$) (Fig. 1B and Fig. S1).Otherwise, BB1 and BB2 didn't show notably high frequency. Given the potential role of BB3 and several compounds showing relatively high score, we focused on 6 compounds (**1a-6b**). The C-terminal end of tripeptide coupled with AOP-HP DNA as a part for conjugation of a small molecule and DNA tag was modified to various types of structure like *N*-methyl amide, ester, free acid. For example, GLP-1R-002 **(1a-1c)**, GLP-1R-032 **(2a-2c)**, and GLP-1R-043 **(6a-6b)** series were diversified through modification of the C-terminal end, which influences efficiency, stability and cellular activity. As a result, total 11 compounds were synthesized as off-DNA compounds based on the high score or frequency ($n > 2$) and used for hit validation (Fig. 1C, Fig. S2-S23).

Combined with DEL screening, we aimed to obtain a more diverse set of compounds through similarity analysis in chemical Bank (Korean Chemical Bank, KCB). Similarity-based compound retrieval was performed using the KCB web platform, which provides search and analysis functions for over 750,000 small molecules deposited in the national synthetic compound repository. The results showed a similar structural pattern in the NGS data, in which a specific structure like BB3–1 was

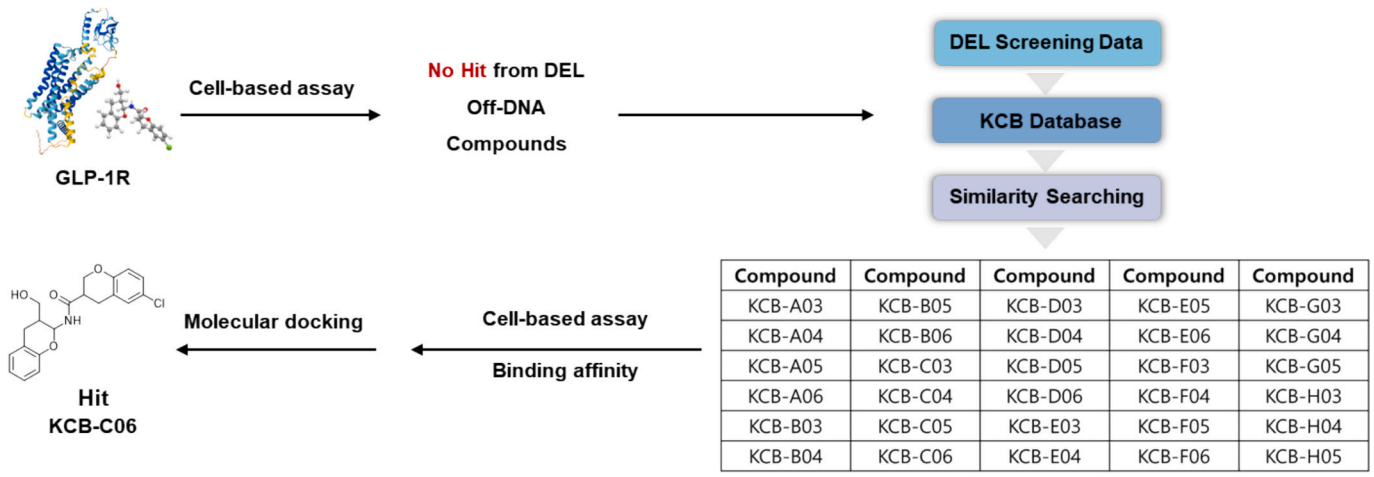

Compound	Compound	Compound	Compound	Compound
KCB-A03	KCB-B05	KCB-D03	KCB-E05	KCB-G03
KCB-A04	KCB-B06	KCB-D04	KCB-E06	KCB-G04
KCB-A05	KCB-C03	KCB-D05	KCB-F03	KCB-G05
KCB-A06	KCB-C04	KCB-D06	KCB-F04	KCB-H03
KCB-B03	KCB-C05	KCB-E03	KCB-F05	KCB-H04
KCB-B04	KCB-C06	KCB-E04	KCB-F06	KCB-H05

Fig. 2. Process of hit validation and analysis of similarity between DEL and Korea Chemical Bank library. Similarity searching was performed by using JChem Base and JChem Cartridge and chemical hashed finger print format of ChemAxon in the KCB web platform.

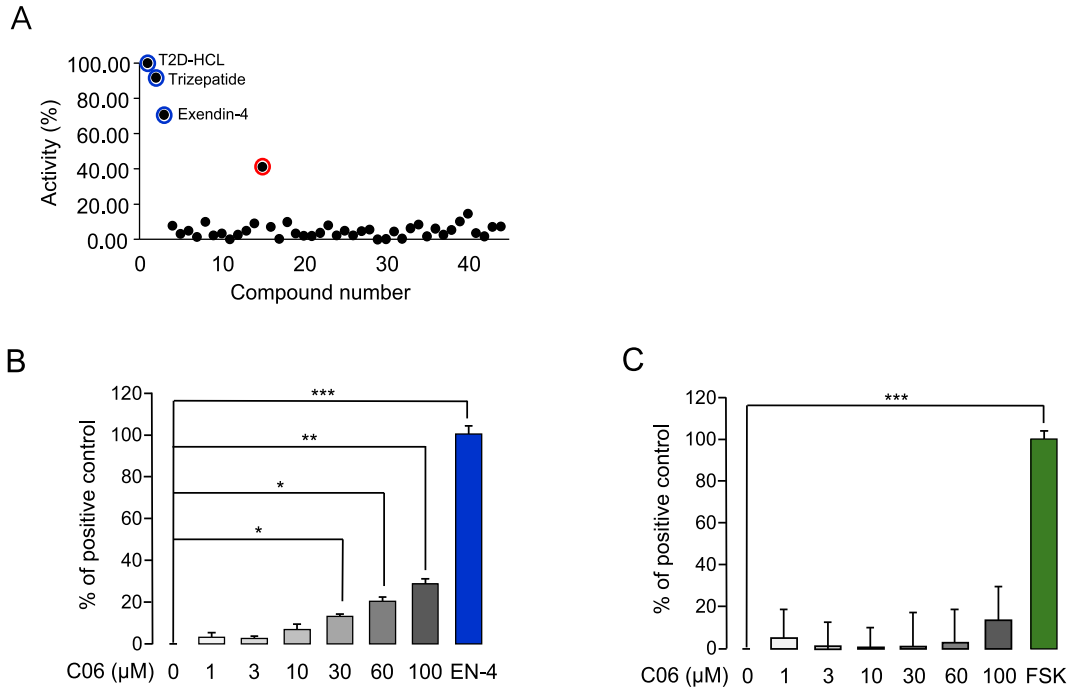

Fig. 3. KCB-C06 enhances the cAMP level in CHO-K1 cells stably expressing GLP-1R. (A) CHO-K1 cells stably expressing GLP-1R were treated with approximately 40 DEL-derived small molecules at the designated screening concentration. (B) Concentration-dependent cAMP production in GLP-1R–overexpressing CHO-K1 cells following treatment with KCB-C06 (0–100 μM). Exendin-4 (10 nM) served as the positive control. (C) Parental CHO-K1 cells lacking GLP-1R were treated with KCB-C06 under the same conditions, and cAMP levels were quantified. Forskolin (10 μM) was used as a control for assay responsiveness. Data represent mean ± SD from three independent experiments performed in triplicate. Statistical significance vs. vehicle: $*p < 0.05$, $**p < 0.01$, $***p < 0.001$.

observed at high frequency value (Fig. 2) [33]. Representatively, the structure with chromane moiety like **KCB-C06** was commonly derived from KCB data. It provides a predictive basis to identify a key structure for binding to GLP-1R. Based on the DEL screening and similarity analysis, KCB compounds were used to evaluate the cellular effects and to predict binding modes of compounds through molecular docking.

3.2. Cell-based GLP-1R enzymatic assay

Selected compounds using DEL technology combined with structure similarity analysis were evaluated for functional activity. Among these, KCB-C06 was identified as the hit compound exhibiting agonistic activity toward GLP-1R (Fig. 3). Concentration–response analysis in CHO-K1 cells overexpressing GLP-1R showed that KCB-C06 induced a dose-dependent increase in intracellular cAMP levels, reaching approximately 30% of the response elicited by the positive control exendin-4 (10 nM) at 100 μM. In contrast, no corresponding response was observed in CHO-K1 cells lacking GLP-1R expression. These findings demonstrate that the signaling response induced by KCB-C06 is GLP-1R-specific and indicate that, although less potent than the reference peptide agonist exendin-4, KCB-C06 functions as a GLP-1R agonist (Fig. 3).

3.3. The functional analysis and binding kinetic assay revealed KCB-C06 as a potential GLP-1R agonist

To characterize the binding kinetics, the biolayer interferometry

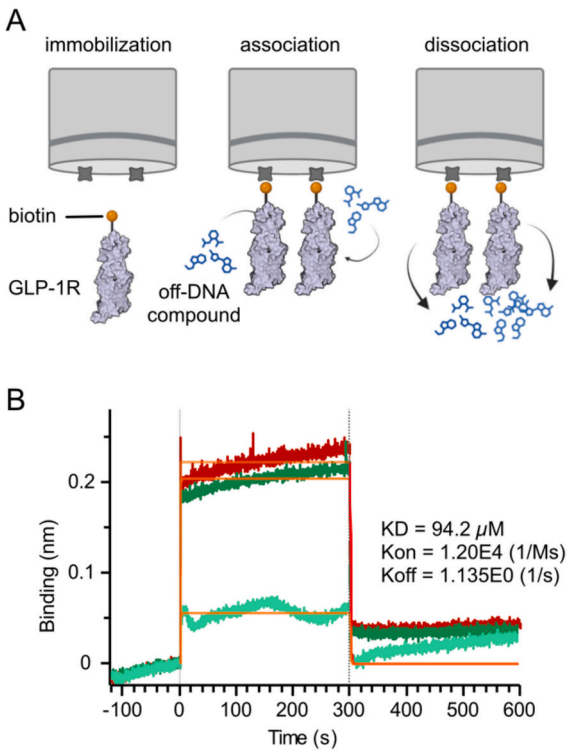

Fig. 4. The binding kinetic study of KCB-C06 on GLP-1R. (A) Schematic representation of biolayer interferometry (BLI) process to measure full kinetic analysis. The processes about immobilization represent the immobilize the biotinylated recombinant GLP-1R on the surface of super streptavidin (SSA) biosensors. The binding kinetics according to the association and dissociation of KCB-C06 compound are represented with the arrow. (B) The sensor gram of KCB-C06 fitted by global fitting (red line). The sensor gram corresponding 25, 100, and 200 μM of KCB-C06 colored by light green, green, and brown, respectively. The calculated KD, Kon, and Koff parameters labeled. (For interpretation of the references to colour in this figure legend, the reader is referred to the web version of this article.)

(BLI) was conducted with the biotinylated recombinant GLP-1R immobilized on super streptavidin sensor (Fig. 4A). According to BLI sensor gram, concentration-dependent increase in signal during the association step indicating direct binding of the KCB-C06 to GLP-1R (Fig. 4B). The global fitting of the association and dissociation curves indicate the dissociation constant (KD) of 94.2 M with a Kon of 1.20×10^4 $M^{-1}S^{-1}$ and a Koff of 1.135 S^{-1} (Fig. 4B). These results suggest that KCB-C06 binds with GLP-1R with modest affinity, primarily driven by a fast off rate. Despite the moderate KD, KCB-C06 is confirmed a capable of direct association with the GLP-1R and shown as the potential initial hit, commonly displaying affinities in the mid-micromolar range.

3.4. Structural basis of KCB-C06 binding mode in orthosteric binding pocket of GLP-1R

To understand the structural mechanism of potential activity of KCB-C06, the structure of GLP-1R was predicted under diffusion-based prediction tool, chai-1 (Fig. S24A) [23]. The overall structure was validated as pDDLT score and overall predicted template modeling (pTM) score as 0.7463 (Fig. S24A and B). The chai-1 predicted model showed structurally similar with crystal structure of apo form full-length GLP-1R (PDB ID 6LN2) [28] as having RMSD with 1.039 Å (Fig. S25A). In contrast to the globally conserved structural feature, the sixth transmembrane helix (TM6) of chai-1 modeled GLP-1R adopts an open structure, rather than the closed arrangement in crystal structure in inactive conformation (Fig. S25B). Structural comparison between the chai-1 modeled GLP-1R and the cryoEM structure (PDB ID 6X18) [34] in complex with glucagon peptide revealed a high degree of global similarity with an RMSD of 1.093 Å across 149 matched Ca atoms (Fig. S25C). Despite the global similarity, the notable local structural deviations were observed in the extracellular domain of GLP-1R (Fig. S25C). Unlike the structural divergence in extracellular part, the TM6 of modeled structure adopt the similar structural arrangement with active conformation of GLP-1R (Fig. S25D). These results collectively suggest that the AI based modeled GLP-1R adopt open and active conformation.

To predict the accurate binding mode of KCB-C06, the complex structure was then modeled with coFold method with chai-1 software. The coFold modeled GLP-1R in complex with both orfoglipron and danuglipron, which are the known small-molecule GLP-1R agonists, showed large difference with its experimental structures (Fig. S26A and B) [24,35]. The rigid body docking simulation of both orfoglipron and danuglipron against the chai-1 modeled structure also showing large difference with its experimental structures (Fig. S26C and D). The docking simulation by using experimental structure showed closely matched binding mode of danuglipron. (Fig. S26E). For danuglipron, the predicted docking pose was nearly identical to the ligand binding environment in cryoEM structure (Fig. S26E and F). These results collectively demonstrated that the accurate prediction of ligand binding mode is highly dependent on the use of receptor structure.

The binding modes of KCB-C06 were predicted as in the orthosteric binding pockets in GLP-1R (Fig. 5A). The binding pocket is constructed with the residues, S31, L32, W33, W203, L217, Q221, F381, and F385 (Fig. 5B and D). The dual faced chromane moiety interact with hydrophobic residues, W33, F381, F385, and W203 by π-stacking interaction (Fig. 5B and D). The peptide bond linking two chromane moieties engages in backbone interaction with residues S31 and L32 of GLP-1R (Fig. 5D). The comparative analysis of KCB-C06 interaction with that of danuglipron revealed a shared set of key interaction residues, L32, W33, W203, L217, and F381 (Fig. 5D and Fig. S26F). These results indicate that KCB-C06 sit in a binding pocket which partially overlap with, but is not identical to, the danuglipron binding site. This observation provides a structural basis for its ability to activate GLP-1R.

4. Discussion

During 3D analysis for selection of the off-DNA compounds, BB3–1 with a chromane moiety showed a high frequency value. Although compounds derived from DEL did not show cellular activity, a structure with a chromane moiety from the similarity data of KCB showed activity, indicating the possibility of acting as a GLP-1R agonist. This result suggested that specific building block structures such as the chromane moiety identified from DEL screening and similarity data of KCB have potential as key binders to GLP-1R. Further hit validation showed the possibility of discovering a small molecule–based hit via DEL screening and data analysis based on high score, frequency, and similarity.

Consistent with these structural observations, cell-based functional assays were performed to evaluate the activity of KCB-C06. In cAMP accumulation assays, KCB-C06 induced a concentration-dependent increase in intracellular cAMP levels in GLP-1R–expressing cells, whereas no activity was observed in parental CHO-K1 cells lacking GLP-1R expression. These results clearly demonstrate that the observed activity of KCB-C06 is mediated by specific activation of GLP-1R rather than nonspecific cellular effects. Although the maximal response produced by KCB-C06 was lower than that of the reference peptide agonist exendin-4, the receptor-specific signaling observed in this study supports the classification of KCB-C06 as a functional GLP-1R agonist and highlights its potential as an initial small-molecule hit for further optimization.

The binding mode prediction of ligands on GLP-1R is highly dependent on the receptor structures used. Only the use of the experimental structure (PDB ID 7LCJ) recapitulated the accurate binding mode of a known ligand (Fig. S26). Therefore, further docking simulations of off-DNA compounds from DEL screening as well as the KCB hit compound

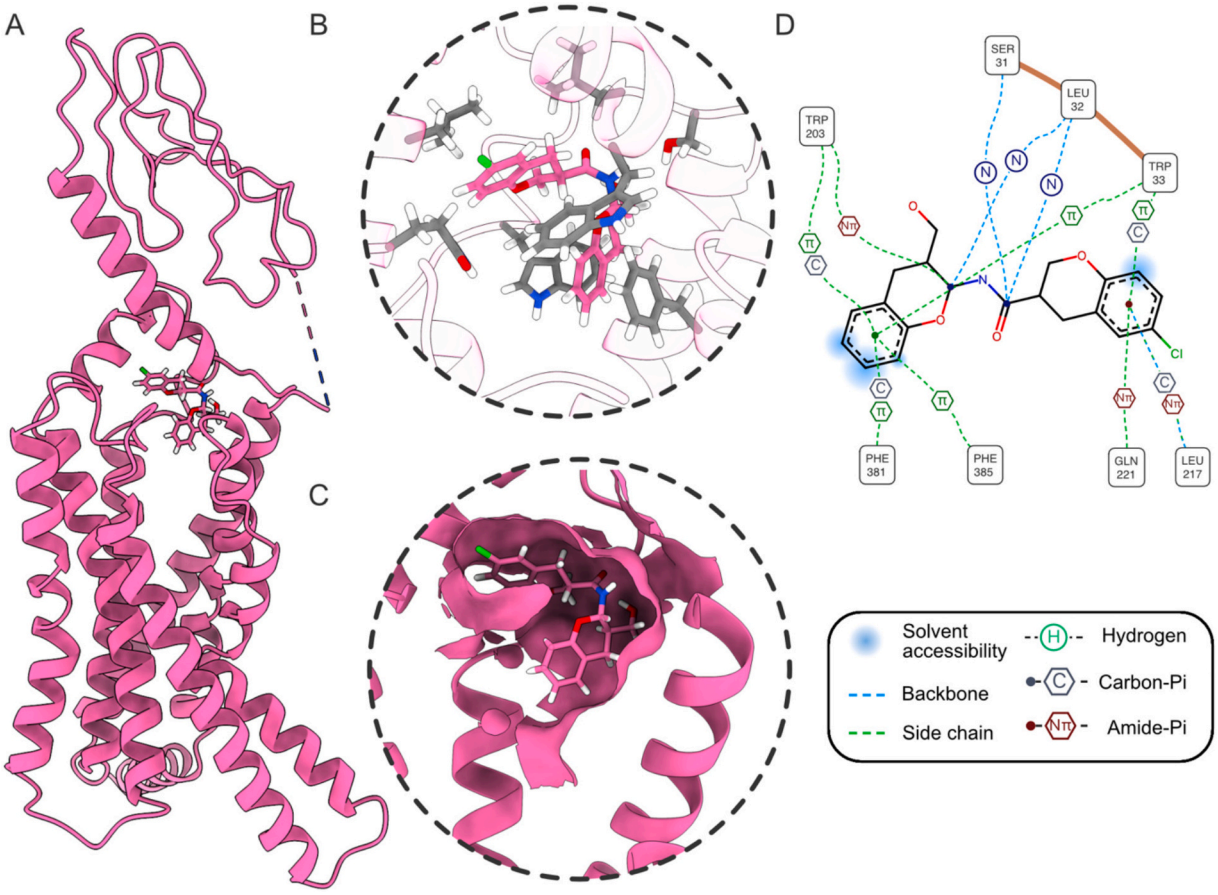

Fig. 5. Structural characterization and binding mode of KCB-C06 in GLP-1R. (A) Overall view of the cryo-EM–derived GLP-1R structure used for docking, shown in ribbon representation (magenta). The predicted binding pose of KCB-C06 is displayed in stick representation within the orthosteric pocket. (B) Close-up view of the predicted binding mode of KCB-C06. The ligand (magenta) and key surrounding receptor residues (grey) are shown in sticks, highlighting the spatial orientation and local microenvironment of the predicted pose. (C) Surface representation of the binding pocket showing how KCB-C06 fits into the receptor cavity. The ligand is shown in sticks to illustrate surface complementarity and potential hydrophobic enclosure. (D) Two-dimensional interaction map summarizing predicted ligand–receptor interactions, including hydrogen bonds, backbone contacts, carbon–π, amide–π, and side-chain–mediated interactions. Solvent accessibility is indicated by blue shading. (For interpretation of the references to colour in this figure legend, the reader is referred to the web version of this article.)

(KCB-C06) were conducted using the experimental structure of GLP-1R (PDB ID 7LCJ) (Fig. S27). While our integrated computational approach provides structural evidence for the orthosteric binding of KCB-C06, static representations are limited in their ability to fully capture the highly dynamic nature of the GLP-1R activation process. Our simulations demonstrated that although AI-based tools such as Chai-1 successfully predict global active conformations, they may lack the local side-chain precision required to recapitulate exact ligand-binding modes without experimental guidance. Consequently, comprehensive molecular dynamics (MD) simulations are essential to overcome these static snapshots. These future studies will be necessary to elucidate the thermodynamic stability of the KCB-C06–receptor complex and the specific conformational transitions induced by this small-molecule agonist. Although the coFold-modeled structure showed globally conserved active conformations, the local diversity between structures—including the apo form (PDB ID 6LN2) [28], peptide-activated form (PDB ID 6X18) [34], orfoglipron-bound form (PDB ID 6XOX) [35], and danuglipron-bound form (PDB ID 7LCJ)[24]—may have distinct binding pockets and restrict the prediction of accurate binding modes. These small structural differences hinder prediction of accurate binding modes of hit compounds as well as identification of novel agonists via structure-based virtual screening (SBVS). The current study demonstrated that the use of AI-based GLP-1R structures for identification of novel drug candidates via SBVS has potential pitfalls due to structural complexity. Hence, exploration of large chemical space through DEL screening methods overcomes the limitations of computational approaches. Although most off-DNA compounds from DEL screening were functionally inactive in cell-based functional analyses, similarity search combined with functional and biophysical analyses finally identified a dual chromane compound linked by a peptide bond as a potential GLP-1R agonist (Figs. 4 and 5). To improve the accuracy of the predicted binding mode of KCB-C06, we performed docking simulations using a receptor model derived from the trimmed cryo-EM GLP-1R structure (Fig. 5).

In this study, DEL-based screening was used for discovery of novel small-molecule agonists targeting GLP-1R. Unfortunately, no hit compound was identified when only DEL screening data and off-DNA synthesis with high score and frequency values were used. While DNA-encoded libraries have several advantages such as large size and structural diversity, they also have limitations such as identification of compounds as binders to the target rather than agonists or binders with low activity. We therefore applied DEL screening data and the Korea Chemical Bank (KCB) database to similarity search to expand the range of small molecules for hit discovery. As a result, KCB-C06 was identified as a hit from similarity search with moderate binding affinity and activity. This result suggests that combining DEL screening with computational tools such as similarity search may facilitate identification of hit compounds containing key structural features. However, KCB-C06 showed relatively low activity compared to a known agonist such as exendin-4. Given that KCB-C06 exhibits only moderate cellular activity

and binding affinity as an initial hit, subsequent structure–activity relationship (SAR) studies will be essential for optimization toward a lead-like GLP-1R agonist. In this context, establishing an accurate binding mode at the early discovery stage is critical for guiding rational design of novel GLP-1R agonists. Collectively, this study not only identifies a new hit compound from DEL screening and similarity search but also provides a conceptual framework underscoring the importance of structure-guided strategies in GLP-1R agonist development.

The identification of novel small-molecule agonists such as KCB-C06 is particularly significant given the expanding therapeutic landscape of GLP-1R signaling. Beyond its established role in glucose homeostasis and metabolic regulation, recent evidence highlights the multi-organ impact of GLP-1R activation, including potent immune cell modulation and psychotropic effects. Specifically, GLP-1R agonists have been shown to exert anti-inflammatory actions across various tissues by modulating innate and adaptive immune responses [36]. Furthermore, the reach of GLP-1R signaling into the central nervous system suggests broad potential for treating neuropsychiatric and neurodegenerative disorders, where these agonists influence reward processing and neuroprotection [37]. The discovery of KCB-C06 through DEL-based screening thus provides a foundation for development of next-generation agonists that could be optimized for these diverse clinical applications.

These results suggest that KCB-C06 represents a small-molecule GLP-1R agonist identified through DEL-based screening and similarity search, providing a foundation for further optimization and characterization.

CRediT authorship contribution statement

Ju Ho Lee: Writing – original draft, Visualization, Validation, Software, Methodology, Investigation, Data curation, Conceptualization. **Doyoun Kim:** Writing – review & editing, Writing – original draft, Visualization, Software, Methodology, Investigation. **Hyejin Jeon:** Writing – review & editing, Writing – original draft, Visualization, Software, Methodology, Investigation. **Sung Bum Park:** Writing – original draft, Methodology, Investigation. **Byumseok Koh:** Writing – original draft, Visualization, Validation, Supervision, Software, Methodology, Investigation, Formal analysis, Data curation, Conceptualization. **Byungho Lim:** Writing – original draft, Methodology, Investigation, Conceptualization. **Kyeong A. Lee:** Formal analysis, Investigation, Methodology, Writing – review & editing. **Kyoung Jin Choi:** Writing – review & editing, Writing – original draft, Methodology, Investigation. **Seong Soon Kim:** Writing – review & editing, Writing – original draft, Resources, Project administration, Methodology, Investigation. **Yujin Kwon:** Writing – original draft, Methodology, Investigation. **Jung-Hee Lim:** Writing – original draft, Software, Resources, Methodology, Investigation. **Jung Hyun Jo:** Writing – original draft, Methodology, Investigation. **Yeonji Park:** Writing – original draft, Methodology, Investigation. **Sunjong Yu:** Writing – original draft, Resources, Methodology, Investigation. **Nam-Chul Cho:** Writing – original draft, Validation, Data curation, Conceptualization. **Wan Namkung:** Writing – review & editing, Writing – original draft, Methodology, Investigation, Formal analysis, Data curation, Conceptualization. **Yuno Lee:** Writing – original draft, Funding acquisition, Data curation, Conceptualization. **Hyun Jin Kim:** Writing – original draft, Investigation, Funding acquisition, Data curation, Conceptualization. **Ki Young Kim:** Writing – original draft, Funding acquisition, Data curation, Conceptualization. **Jung-Nyoung Heo:** Writing – review & editing, Writing – original draft, Supervision, Project administration, Investigation, Funding acquisition, Data curation, Conceptualization.

Declaration of competing interest

The authors declare the following financial interests/personal relationships which may be considered as potential competing interests: Jung-Nyoung Heo reports financial support was provided by Korea Research Institute of Chemical Technology. Jung-Nyoung Heo reports financial support was provided by National Research Foundation of Korea. If there are other authors, they declare that they have no known competing financial interests or personal relationships that could have appeared to influence the work reported in this paper.

Acknowledgements

This research was supported by the Bio & Medical Technology Development Program of the National Research Foundation (NRF-RS-2023-00235550) and the Korea Research Institute of Chemical Technology (KK2531–10, KK2633–30) of Republic of Korea. The chemical library and data used in this study were kindly provided by Korea Chemical Bank (www.chembank.org) of Korea Research Institute of Chemical Technology.

Appendix A. Supplementary data

Supplementary data to this article can be found online at https://doi.org/10.1016/j.rechem.2026.103415.

Data availability

Data will be made available on request.

References

[1] J.E. Campbell, et al., GIPR/GLP-1R dual agonist therapies for diabetes and weight loss—chemistry, physiology, and clinical applications, Cell Metab. 35 (9) (2023) 1519–1529.
[2] R. Carlessi, et al., GLP-1 receptor signalling promotes β-cell glucose metabolism via mTOR-dependent HIF-1α activation, Sci. Rep. 7 (1) (2017) 2661.
[3] M.A. Burmeister, et al., The hypothalamic glucagon-like peptide 1 receptor is sufficient but not necessary for the regulation of energy balance and glucose homeostasis in mice, Diabetes 66 (2) (2017) 372–384.
[4] B.J. Lamont, et al., Pancreatic GLP-1 receptor activation is sufficient for incretin control of glucose metabolism in mice, J. Clin. Invest. 122 (1) (2012) 388–402.
[5] H.J. Wong, et al., Efficacy of GLP-1 receptor agonists on weight loss, BMI, and waist circumference for patients with obesity or overweight: a systematic review, meta-analysis, and meta-regression of 47 randomized controlled trials, Diabetes Care 48 (2) (2025) 292–300.
[6] G. Bendotti, et al., The anti-inflammatory and immunological properties of GLP-1 receptor agonists, Pharmacol. Res. 182 (2022) 106320.
[7] J.R. Ussher, et al., Inactivation of the cardiomyocyte glucagon-like peptide-1 receptor (GLP-1R) unmasks cardiomyocyte-independent GLP-1R-mediated cardioprotection, Molecular Metab. 3 (5) (2014) 507.
[8] J. Seufert, B. Gallwitz, The extra-pancreatic effects of GLP-1 receptor agonists: a focus on the cardiovascular, gastrointestinal and central nervous systems, Diabetes. Obes. Metab. 16 (8) (2014) 673–688.
[9] C. Hölscher, Protective properties of GLP-1 and associated peptide hormones in neurodegenerative disorders, Br. J. Pharmacol. 179 (4) (2022) 695–714.
[10] T. Okerson, R.J. Chilton, The cardiovascular effects of GLP-1 receptor agonists, Cardiovasc. Ther. 30 (3) (2012) e146–e155.
[11] F.K. Saraiva, A.C. Sposito, Cardiovascular effects of glucagon-like peptide 1 (GLP-1) receptor agonists, Cardiovasc. Diabetol. 13 (1) (2014) 142.
[12] A.L. Satz, et al., DNA-encoded chemical libraries, Nat. Rev. Methods Primers 2 (1) (2022) 3.
[13] R.M. Franzini, D. Neri, J. Scheuermann, DNA-encoded chemical libraries: advancing beyond conventional small-molecule libraries, Acc. Chem. Res. 47 (4) (2014) 1247–1255.
[14] J.H. Lee, et al., Discovery of CA9–005 as a new carbonic anhydrase 9 inhibitor using a DNA encoded-libraries, Results. Chem. (2025) 102455.
[15] L. Mannocci, et al., High-throughput sequencing allows the identification of binding molecules isolated from DNA-encoded chemical libraries, Proc. Natl. Acad. Sci. 105 (46) (2008) 17670–17675.
[16] J. Scheuermann, et al., DNA-encoded chemical libraries, J. Biotechnol. 126 (4) (2006) 568–581.
[17] R.E. Kleiner, C.E. Dumelin, D.R. Liu, Small-molecule discovery from DNA-encoded chemical libraries, Chem. Soc. Rev. 40 (12) (2011) 5707–5717.
[18] M.A. Clark, Selecting chemicals: the emerging utility of DNA-encoded libraries, Curr. Opin. Chem. Biol. 14 (3) (2010) 396–403.
[19] A.A. Peterson, D.R. Liu, Small-molecule discovery through DNA-encoded libraries, Nat. Rev. Drug Discov. 22 (9) (2023) 699–722.
[20] P. Dickson, DNA-encoded library technology— a catalyst for covalent ligand Discovery, ACS Chem. Biol. 19 (4) (2024) 802–808.

[21] A. Gironda-Martínez, et al., DNA-encoded chemical libraries: a comprehensive review with succesful stories and future challenges, ACS Pharmacology & Translational Science 4 (4) (2021) 1265–1279.
[22] Y. Song, X. Li, Evolution of the selection methods of DNA-encoded chemical libraries, Acc. Chem. Res. 54 (17) (2021) 3491–3503.
[23] C. Discovery, et al., Chai-1: Decoding the molecular interactions of life, bioRxiv (2024).
[24] X. Zhang, et al., Evolving cryo-EM structural approaches for GPCR drug discovery, Structure 29 (9) (2021) 963–974 e6.
[25] O. Trott, A.J. Olson, AutoDock Vina: improving the speed and accuracy of docking with a new scoring function, efficient optimization, and multithreading, J. Comput. Chem. 31 (2) (2010) 455–461.
[26] OneAngstrom, SAMSON (Interaction Designer Extension), OneAngstrom, 2025.
[27] A. Vangone, et al., Large-scale prediction of binding affinity in protein-small ligand complexes: the PRODIGY-LIG web server, Bioinformatics 35 (9) (2019) 1585–1587.
[28] F. Wu, et al., Full-length human GLP-1 receptor structure without orthosteric ligands, Nat. Commun. 11 (1) (2020) 1272.
[29] E.C. Meng, et al., UCSF ChimeraX: tools for structure building and analysis, Protein Sci. 32 (11) (2023) e4792.
[30] M. Varadi, et al., AlphaFold protein structure database: massively expanding the structural coverage of protein-sequence space with high-accuracy models, Nucleic Acids Res. 50 (D1) (2022) D439–D444.
[31] M. Varadi, et al., AlphaFold protein structure database in 2024: providing structure coverage for over 214 million protein sequences, Nucleic Acids Res. 52 (D1) (2024) D368–D375.
[32] J. Jumper, et al., Highly accurate protein structure prediction with AlphaFold, nature 596 (7873) (2021) 583–589.
[33] O. Laufkötter, T. Miyao, J. Bajorath, Large-scale comparison of alternative similarity search strategies with varying chemical information contents, ACS Omega 4 (12) (2019) 15304–15311.
[34] X. Zhang, et al., Differential GLP-1R binding and activation by peptide and non-peptide agonists, Mol. Cell 80 (3) (2020) 485–500 e7.
[35] T. Kawai, et al., Structural basis for GLP-1 receptor activation by LY3502970, an orally active nonpeptide agonist, Proc. Natl. Acad. Sci. U. S. A. 117 (47) (2020) 29959–29967.
[36] M. Ben Nasr, et al., Glucagon-like peptide 1 receptor is a T cell-negative costimulatory molecule, Cell Metab 36 (6) (2024) 1302–1319.e12.
[37] L. Bucciarelli, et al., Psychotropic effects of GLP-1R agonists, Pharmacol Res 222 (2025) 108036.